ELSEVIER

27 January 1995

Chemical Physics Letters 232 (1995) 524–530

CHEMICAL PHYSICS LETTERS

Time-dependent Monte Carlo simulations of radical densities and distributions on the diamond{001}(2×1):H surface

E.J. Dawnkaski, D. Srivastava, B.J. Garrison

Department of Chemistry, The Pennsylvania State University, University Park, PA 16802, USA

Received 12 August 1994; in final form 14 November 1994

Abstract

Time-dependent Monte Carlo simulations are performed to determine the steady state distribution and density of C radicals on the diamond {001}(2×1):H surface. The required reaction rates and probabilities of the individual events are either explicitly calculated via molecular dynamics simulations or taken directly from experiments. Each simulation time step is equivalent to a real time step in which all particles are simultaneously allowed to move, albeit probabilistically. The calculations show the presence of two chemically distinct surface bonding environments. In addition to structurally isolated radical sites we also find strained and reactive π bonds (diradicals) on the surface.

1. Introduction

Computer simulations of the structure and dynamics of materials concentrate mainly on either the microscopic evolution of a system, typically less than a few nanoseconds (1 ns $= 10^{-9}$ s) in duration, or the equilibrium structure and properties of the system in the steady state. For instance, molecular dynamics (MD) computer simulations are often used to determine the microscopic motions of a system as a function of time and predict the associated microscopic mechanisms. Due to very small time steps ($\sim 10^{-15}$ s) and the simulation cell size constraints ($\sim (100$ Å$)^3$) MD simulations cannot describe the macroscopic properties of the system that evolve over longer periods of time and larger size domains. On the other hand techniques such as Monte Carlo (MC) simulations predict steady state properties and structures at the expense of the microscopic details of the time-dependent dynamics. There have been recent attempts to bridge the chasm between the two approaches by way of kinetic [1–5] and time-dependent [6–12] Monte Carlo methods. These MC methods include the retention of the microscopic dynamics through the rates and probabilities of predetermined microscopic processes and yet overcome the time and size constraints typical of the MD methods. Consequently these MC methods allow access to both the microscopic regime of MD simulations and the macroscopic regime of conventional MC simulations. There have been two significant developments as these MC methods have evolved toward the realistic simulation of dynamic systems. First, the quality of the calculated energetics of the system has greatly improved for both the equilibrium configurations and the transition state barriers [1,3,10–12]. Therefore it is possible to use methods like transition state theory to calculate the rates of individual microscopic processes or reactions [10–12]. Second, the definition of the MC time step and its relationship to real experimental time has been rigorously sought [6–12]. In the case of an individual isolated process the real time required for a reaction to occur is related to the inverse of the reaction

0009-2614/95/$09.50 © 1995 Elsevier Science B.V. All rights reserved
SSDI 0009-2614(94)01393-4

rate, and the MC time step is set equal to this quantity [10–12]. For a many-particle, multi-process system, however, the correlation between the MC time step and real time is not so easily elucidated. One approach in this regard has been to simply scale the MC time step by a normalization constant such that the experimental time scale is matched [1–5]. More complex approaches involve assigning to each particle in the system independent time steps in a manner similar to the case of the isolated process, and the real time step is represented by an average over all of the independent time steps [6–9].

In this Letter, a simple alternative to the real time problem is presented. Given a set of realistic rates for all the processes in a system, any constant time step that is less than the duration of the fastest process may be chosen. This time step calibrates the real time as will be explained below. All particles are allowed to move in a single time step. The individual processes or reactions are randomly selected but are accepted or rejected with a probability which is simply a product of the chosen time step and the rate of the individual process. This many-particle, multi-process time-dependent Monte Carlo (TDMC) method, is used to create a dynamical picture of the diamond {001}(2×1):H surface under hot filament, chemical vapor deposition (CVD) growth conditions. The growth environment is a gaseous hydrocarbon atmosphere at total pressures of 20–30 Torr in which CH_3 radicals and C_2H_2 molecules are present in small quantities, typically mole fractions of 10^{-3} or less [13]. The gas phase H atoms are in dynamic equilibrium with the diamond surface such that the C radicals on the surface are continuously created and destroyed by H abstraction and adsorption, H_2 desorption, and the reverse of these processes. The equilibrium density and distribution of the C radicals at a given diamond surface and the gas temperature are important for any mechanistic understanding of the diamond growth process at that surface. The required reaction rates and probabilities for the H and H_2 reactions with the diamond {001}(2×1):H surface are either explicitly calculated by way of MD or transition state theory (TST) methods or taken directly from experiments. The TDMC method is used to predict the density and distribution of carbon radicals on the diamond{001}(2×1):H surface in a gaseous H atmosphere. The simulated equilibrium radical densities in a pure hydrogen environment [1] on the diamond{001}(2×1):H surface for the temperature range of 1200 to 1800 K are found to be 4% to 34%, respectively. More importantly, we predict that 4% (at 1200 K) to 34% (at 1800 K) of the radicals are paired up at surface dimers, a situation that is formally equivalent to the formation of π bonds. The prediction of a second type of reaction center, namely strained π bonds, may provide an alternative site for CH_3 adsorption and hence for the initiation of film growth. A simple estimation of the formation of the CH_2 adspecies at a dimer site through adsorption at a π bond is given and indicates that the reaction at the π bond is four to six orders of magnitude faster than the reaction at an isolated radical site. In Section 2, the method and details of the calculation are presented, and in Section 3 we discuss the main results of this work.

2. Method

The theoretical approach which we have been recently developing combines molecular dynamics simulations for extracting reaction probabilities and mechanisms [15], transition state theory for determining reaction rates of activated processes [10], and time-dependent Monte Carlo calculations for extrapolating the short-time microscopic information to the time scales and macroscopic regime of experimental conditions [11,12]. The CVD experimental process involves numerous individual reactions that occur between the gas phase species, the substrate and intermediate surface species. Since it is at best difficult to experimentally measure (or even identify) the rate or probability of each of the individual reactions involved, one strategy is to model the growth processes with reaction rates and probabilities that are typically abstracted from the gas phase hydrocarbon literature [16]. This approach, however, assumes that all gas phase rates are transferable to the respective surface rates for each of the processes involved. We, therefore, have used either values taken from diamond surface experiments or explicitly calculated the rates of each process using a many-body reactive hydrocarbon interaction potential [17,18]. This potential was originally

[1] CVD conditions typically utilize >99% hydrogen and <1% hydrocarbons – see for example, Ref. [14].

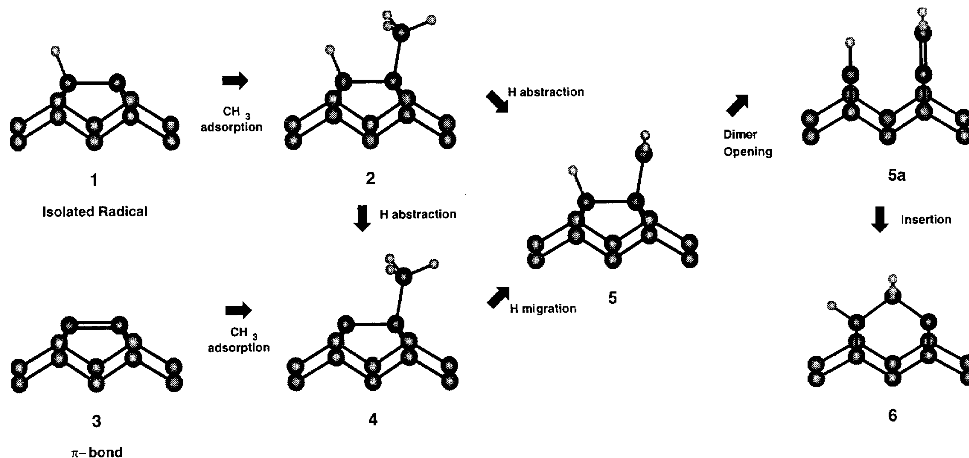

Fig. 1. Representation of atomic configurations for a surface dimer (darker spheres) and surrounding neighbor atoms (lighter spheres). The C atom of the adsorbed species is also darker in color and the H atoms are represented by small spheres. Each scheme has different adsorbates on the surface dimer. (**1**) H and isolated radical; (**2**) H and CH_3; (**3**) π-bond; (**4**) isolated radical and CH_3; (**5**) H and CH_2; (**5a**) H and CH_2, ethylenic configuration; (**6**) CH_2 inserted into the surface dimer.

developed to model the chemical vapor deposition of diamond films but, in fact, has been used in a number of simulations of other hydrocarbon interactions and reactions including the insertion of CH_2 into a surface dimer on the diamond {001}(2×1)H surface [15]; molecular reactions during sputtering [19]; and reaction [20–22] at diamond surfaces.

Each surface C atom in the diamond {001}(2×1) dimer reconstructed surface has threefold coordination with two C atom neighbors in the second layer and one in the first layer (configuration **3** in Fig. 1). The two adjacent first layer C atoms form a dimer bond which on the clean surface has considerable π character [23–25]. The abundance of atomic H in most environments appropriate to CVD diamond growth forces the majority of the surface C atoms, however, to also be bonded to a H atom (configuration **1** in Fig. 1). The surface C atoms in this case have fourfold coordination albeit distorted from a perfect tetrahedral geometry. In order to model the properties of radicals on this surface in equilibrium with gas phase H atoms, the probabilities of H atom adsorption, desorption, and abstraction; H_2 desorption and adsorption and radical diffusion must be determined. The evaluation of each of these quantities is briefly discussed below.

MD simulations are used to determine both the probability of H atom adsorption (surface radical annihilation) and the probability of surface H atom abstraction by a gas phase H atom to form gaseous H_2 (surface radical formation) in a manner identical to that used for the diamond {111} surface [21,22,26]. Separate calculations are performed for single radicals and π-bond sites. In addition, the reverse reaction of a H_2 molecule depositing a single atom at a surface radical has been estimated from the abstraction reaction energetics [27]. The collision rates of H atoms and H_2 molecules with the surface have been calculated using partial pressures of 0.1 and 18 Torr, respectively [28]. The mechanism of thermal desorption of hydrogen from the {001}(2×1):H surface is not very well understood [29,30], but is definitely too slow to be modeled with MD. This quantity has thus been estimated from the experimental thermal desorption data of Thomas et al. [31] for molecular desorption probabilities. We require that the two H atoms that form the gaseous H_2 molecule arise from one surface dimer but make no assumptions about the microscopic desorption mechanism. The reverse process under similar conditions is estimated from the relative energetics. The probability of a H_2 molecule depositing either one or two H atoms is several orders of magnitude lower than the probability of H atom adsorption so the precise values are relatively unimportant.

The lateral surface diffusion of radicals is assumed to occur through uncorrelated hops of surface H atoms onto radical sites with the rate constants for these hops

Table 1
Probabilities of H atom dynamics on the diamond {001} (2×1):H surface

Reaction	ν (s^{-1})	E_{act} (eV)	Probability in δt [a]		
			1200 K	1500 K	1800 K
H atom collision (0.1 Torr)			6.56×10^{-3}	5.87×10^{-3}	5.36×10^{-4}
H atom adsorption [b]					
at an isolated C radical			3.48×10^{-3}	3.20×10^{-3}	2.31×10^{-4}
at one C atom in π bond			5.11×10^{-3}	4.51×10^{-3}	3.96×10^{-4}
H atom desorption					
to form an isolated radical	1.00×10^{13}	4.43	2.49×10^{-13}	1.31×10^{-9}	3.96×10^{-7}
to form π bond	1.00×10^{13}	3.43	3.94×10^{-9}	3.00×10^{-6}	2.50×10^{-5}
H atom abstraction [b]					
to form an isolated radical			1.44×10^{-4}	3.18×10^{-4}	4.47×10^{-5}
to form π bond			2.07×10^{-4}	3.56×10^{-4}	5.12×10^{-5}
H_2 deposition of a H atom [c]					
at an isolated radical			2.60×10^{-5}	1.07×10^{-4}	2.28×10^{-5}
at one C atom in π bond			4.68×10^{-9}	9.06×10^{-8}	6.54×10^{-8}
H_2 desorption	1.00×10^{13}	3.14	6.51×10^{-8}	2.82×10^{-5}	1.62×10^{-4}
H_2 adsorption			1.90×10^{-14}	8.43×10^{-11}	2.22×10^{-10}
hop to a radical site					
across dimer	3.18×10^{13}	2.06	7.09×10^{-3}	3.81×10^{-1}	5.43×10^{-1}
across trough	3.62×10^{13}	2.88	2.90×10^{-6}	7.61×10^{-4}	3.12×10^{-3}
parallel to trough	1.53×10^{13}	2.50	4.84×10^{-5}	6.10×10^{-3}	1.53×10^{-2}
hop to form a π bond					
across trough	4.13×10^{13}	2.79	7.92×10^{-6}	1.75×10^{-3}	6.37×10^{-3}
parallel to trough	1.63×10^{13}	2.62	1.62×10^{-5}	2.57×10^{-3}	7.53×10^{-3}
hop to break a π bond					
across trough	3.82×10^{13}	3.80	4.20×10^{-10}	6.53×10^{-7}	8.76×10^{-6}
parallel to trough	1.51×10^{13}	3.61	1.04×10^{-9}	1.12×10^{-6}	1.18×10^{-5}

[a] Probability = rate × δt, $\delta t = 10^{-7}$ s at 1200 and 1500 K and $\delta t = 10^{-8}$ s at 1800 K.
[b] H atom abstraction and adsorption probabilities (per site) were calculated from MD simulations. These probabilities were converted into the corresponding rates by using calculated H collision rates with the surface at 0.1 Torr. See Ref. [32].
[c] The H_2 pressure is assumed to be 18 Torr.

determined by simplified TST [10–12]. Three H atom diffusion mechanisms are considered – migration across the surface dimer, migration across the trough between two dimer rows and migration parallel to the dimer rows. The first mechanism, migration across the surface dimer, leads to no real net motion, but it is included for completeness. Separate rates have been determined for H atom jumps both to a single radical site and to a π bond (diradical site) as the π bond is more stable by 1 eV than two isolated and non-interacting radicals using this interaction potential. The temperature-dependent TST rate constant is given by $k_{TST} = \nu \exp(-E_{act}/k_B T)$. The prefactor, ν, and the activation energy, E_{act}, are calculated from the interaction potential and are given in Table 1. An explanation of the relative values for single radicals and π bonds and the relative differences between the dynamics on {001} and {111} surfaces will be discussed elsewhere.

Since we are considering a variety of competing processes for many particles simultaneously, an important consideration is the method by which we extend the Monte Carlo calculation into the time domain. For a single-particle, multi-process system our approach has been to use the rates of the microscopic processes to determine the duration of the processes. There is only one clock which keeps track of time for the entire system [10–12]. The rates of all of the allowed processes for the particle are combined to obtain a total rate and the time step in which the particle moves is then the inverse of the total rate. At each time step, one of all the possible processes is randomly selected and the

selected process is allowed to occur with a probability which is the product of the time step and the rate of the individual process [10–12]. The rates of the individual processes are thus included only through the probabilities in a single time step which is the real time itself. Since the processes are randomly selected both the rare and frequent events are uniformly sampled at each step although the probability of the rare events occurring is very small. The method has been applied successfully to the case of Si adatom diffusion on Si and Ge surfaces [11,12]. In this Letter, we extend this method [11,12] to a many-particle, multi-process system. The extension is based upon the observation that given the rate of each individual process in a system, the probability of a process occurring within *any* specified time period or time step is simply the product of the time step and the rate for the process. A single constant time step, δt, for the overall dynamics is chosen such that it is less than the duration of the fastest process considered. The probabilities for all of the considered processes are thus between 0 and 1. All of the particles are allowed to move in each step with the process for each particle randomly selected. A particle moves, however, only if the probability of the move is less than a uniformly sampled random number between 0 and 1. The constant time step is chosen such that the acceptance probability of the fastest process is about 0.5, a value typical of most MC simulations. With this procedure, values of $\delta t = 10^{-7}$ s (1200, 1500 K) and $\delta t = 10^{-8}$ s (1800 K) are chosen.

A comparison of the above method with other recent TDMC approaches for many-particle, multi-process systems [6–9] is now in order. Given the rates and probabilities for each process in the system one approach has been to assign each particle an independent time clock. The clock for each particle advances as the reciprocal of the rate of the process that occurs. A master clock keeps track of the overall time, particles move consecutively such that a particle moves only when sufficient time has passed [6,7]. The relationship between the time kept on individual atomic clocks and on the master clock with real experimental time remains unclear and is considered as an average over all of the particles. The approach in Ref. [8] picks particles randomly, from a list of given transition type, but the relationship of the individual time steps with the overall real time step is also considered as an average over all the particles in the system. In our approach there is only one time which is the real time itself. At each step all particles are allowed to move, albeit probablitically, and events for the particle are randomly sampled. The inconsistencies in the independent and master clock method [6–8] have been identified and addressed in a recent publication [9]. In the refined method [9], for Poisson processes, the transition probabilities are constructed from the normalization of individual rates and the time step is the inverse of the average rate weighted by a Poisson probability distribution. The particles are randomly selected and the time step is incremented only for successful moves. When rare events occur, they are necessarily accompanied by long-time increments. Our method allows for rare events happening at short time duration albeit with small probability. This is in principle closer to the philosophy of static MC methods where atomic configurations of higher energies are also accepted albeit with small probability.

For the diamond surface, a grid of 100×100 points with periodic boundary conditions has been used in which each grid point is a {001}(2×1) surface C atom either with or without a bonded H atom. The time-dependent MC calculation proceeds by keeping track of all the grid points as well as a history of each radical. In a single time step all grid points are checked for the possible adsorption, desorption or abstraction events which affect the radical density. The complete list of radicals is then cycled through and checked for diffusion processes in the same time step. A separation of diffusive events from all the others is assumed in this work, although this is not in general necessary. This assumption is deemed reasonable as the overall radical concentration before and after the diffusion events remains the same. The model allows for tabulation of the overall radical and π-bond concentrations as well as the diffusion constants or lifetimes for each species.

3. Results

The values of each of the computed quantities per MC time step for temperatures of 1200, 1500 and 1800 K are given in Table 1. The experimental growth conditions are in the lower half of this temperature range. The calculation at the higher temperature (1800 K) is included to account for the possibility that the surface diffusion activation barriers obtained from the empiri-

cal potential may be higher than the actual barriers [2]. At 1200 K the most probable single event is H atom adsorption on a radical or π bond. At 1800 K the diffusive events are more probable than adsorption or desorption. Given that all these events are occurring competitively, the time-dependent MC calculation is necessary at all temperatures to determine the macroscopic characteristics of the radical concentration and distribution. The equilibrium radical densities in the temperature range of 1200 to 1800 K are found to be 4% to 34%, respectively, and 4% (at 1200 K) to 34% (at 1800 K) of these are paired up at surface dimers as π bonds. The prediction of a second reaction center, namely, a strained π bond, on the H-diamond {001}(2×1) surface is a direct conclusion from the TDMC calculations. We did not initially calculate rates for π-bond sites but after preliminary TDMC calculations we found it necessary to include them in the table of rates. The lifetimes of two types of reaction sites have also been computed. For the single radical site, the lifetime varies from 22 μs at 1200 K to 38 μs at 1800 K. The π bond has a lifetime of approximately 10 μs and is independent of temperature.

It has been proposed that a key step for diamond film growth is the insertion of a CH_2 species initially adsorbed on one of the surface dimer C atoms into the surface dimer (configurations **5** and **6** of Fig. 1), thus adding one C atom in an epitaxial position [15,33]. If only isolated radicals are present as reaction centers, as previously postulated (see, for example, Refs. [16,34]) the formation of the adsorbed CH_2 unit (configuration **5**) can occur via two pathways as shown in Fig. 1. In path **1–2–5**, adsorption of CH_3 at the isolated radical is followed by H abstraction from the adsorbed CH_3. This leaves the CH_2 primed for insertion into the surface dimer. Alternatively in path **1–2–4–5**, adsorption of CH_3 at the isolated radical is followed by H abstraction from the adjacent surface dimer C atom. An intra- or inter-molecular H migration then takes place from the adsorbed CH_3 to this nascent proximate radical. On the other hand, if strained π bonds are also present on the surface, the CH_3 can add to a π bond (path **3–4–5**) and a H atom can migrate to the resultant adjacent radical by either an intra- or an inter-molecular mechanism. The difference in importance among the paths **1–2–5**, **1–2–4–5** and **3–4–5** depends on the concentrations of the isolated radical (configuration **1**) versus the π bond (configuration **3**), the rates of CH_3 addition to the two reaction centers, and the relative rate of H abstraction (path **2–5** or **2–4**) versus H migration (path **4–5**). The key factor which influences the relative rates among the three reaction paths shown in Fig. 1 is the H abstraction probability in path **2** to **5** or **2** to **4** versus the H migration probability in path **4** to **5**. We estimate that the formation of CH_2 adspecies through the π bond site in scheme **3** is four to six orders of magnitude faster than through the isolated radical in scheme **1**.

In summary, a many-particle, multi-process TDMC calculation with explicitly determined microscopic rates and probabilities has been used to predict the density and distribution of C radicals on the diamond{001}(2×1):H surface under CVD conditions. The simulation time step is the real time step in which all particles are allowed to move simultaneously, albeit probabilistically. Both the rare and frequent events are uniformly sampled as a function of time, although the acceptance probability of the rare events remains very small. The resultant C radical distribution shows the presence of a second form of initial chemical environment for hydrocarbon reactions on this surface. Although π bonds are well established on the clean diamond {001} surface, other than in this work they have seldom been considered [35] as possible reaction centers for diamond film growth under CVD conditions. The TDMC approach thus shows promise as a means of incorporating adsorption and diffusion of hydrocarbon species, reaction events that lead to crystalline growth (and possibly even amorphous growth) into computations, thus bringing microscopic reaction mechanisms to the macroscopic regime. Efforts are underway to extend this prescription to three dimensions in order that diamond growth can be modeled.

[2] The empirical potential is limited to nearest neighbor interactions. Consequently some diffusion events correspond to almost breaking a bond. This would give an artificially large activation energy.

Acknowledgements

We gratefully acknowledge financial support from the Office of Naval Research. We thank Professor Ken S. Feldman for insightful conversations on organic chemistry and diamond film growth processes.

References

[1] Z. Zhang and H. Metiu, Surface Sci. Letters 292 (1993) L781.
[2] P.W. Rooney and F. Hellman, Phys. Rev. B 48 (1993) 3079.
[3] J. Xing and H.L. Scott, Phys. Rev. B 48 (1993) 4806.
[4] J. Cortes, E. Valencia and P. Araya, J. Chem. Phys. 100 (1994) 7672.
[5] S. Pal and D.P. Landau, Phys. Rev. B 49 (1994) 10597.
[6] H.C. Kang and W.H. Weinberg, J. Chem. Phys. 90 (1989) 2824.
[7] L.A. Ray and R.C. Baetzold, J. Chem. Phys. 93 (1990) 2871.
[8] A.M. Bowler and E.S. Hood, J. Chem. Phys. 94 (1991) 5162.
[9] K.A. Fichthorn and W.H. Weinberg, J. Chem. Phys. 95 (1991) 1090.
[10] A.F. Voter, Phys. Rev. B 34 (1986) 6819.
[11] D. Srivastava and B.J. Garrison, J. Chem. Phys. 95 (1991) 6885.
[12] D. Srivastava and B.J. Garrison, Phys. Rev. B 47 (1993) 4464.
[13] F.G. Celii, P.E. Pehrsson, H. Wang and J.E. Butler, Appl. Phys. Letters 52 (1988) 2043.
[14] S.J. Harris and L.R. Martin, J. Mater. Res. 5 (1990) 2313.
[15] B.J. Garrison, E.J. Dawnkaski, D. Srivastava and D.W. Brenner, Science 255 (1992) 835.
[16] S.J. Harris and D.G. Goodwin, J. Phys. Chem. 97 (1993) 23.
[17] D.W. Brenner, Phys. Rev. B 42 (1990) 9458.
[18] D.W. Brenner, J.A. Harrison, C.T. White and R.J. Colton, Thin Solid Films 206 (1991) 220.
[19] R.S. Taylor and B.J. Garrison, J. Am. Chem. Soc. 116 (1994) 4465.
[20] D.W. Brenner, D.H. Robertson, R. Carty, D. Srivastava and B.J. Garrison, MRS Proc. 278 (1992) 255.
[21] X. Chang, D.L. Thompson and L.M. Raff, J. Chem. Phys. 97 (1993) 10112.
[22] X. Chang, M. Perry, J. Peploski, D.L. Thompson and L.M. Raff, J. Chem. Phys. 99 (1993) 4748.
[23] S.H. Yang, D.A. Drabold and J.B. Adams, Phys. Rev. B 48 (1993) 5261.
[24] Y.L. Yang and M.P. D'Evelyn, J. Am. Chem. Soc. 114 (1992) 2796.
[25] Z. Jing and J.L. Whitten, Phys Rev. B 50 (1994) 2598.
[26] D.W. Brenner, D.H. Robertson, R. Carty, D. Srivastava and B.J. Garrison, MRS Proc. 278 (1992) 255.
[27] R.L. Carty, Masters Thesis, Penn State University (1993).
[28] W.L. Hsu, Appl. Phys. Letters 59 (1991) 1427.
[29] A.V. Hamza, G.D. Kubiak and R.H. Stulen, Surface Sci. 237 (1992) 35.
[30] Y.L. Yang, L.M. Ulvick, L.F. Sutcu and M.P. D'Evelyn, Thin Solid Films 225 (1993) 203.
[31] R.E. Thomas, R.A. Rudder and R.J. Markunas, J. Vacuum Sci. Technol. A 10 (1992) 2451.
[32] P.W. Atkins, Physical chemistry, 3rd Ed. (Freeman, New York, 1986) p. 764.
[33] D. Huang and M. Frenklach, J. Phys. Chem. 96 (1992) 1868.
[34] J.E. Butler and R.L. Woodin, Phys. Trans. Roy. Soc. A 342 (1993) 209, and references therein.
[35] S. Skokov, B. Weiner and M. Frenklach, J. Phys. Chem. 98 (1994) 8.